

available at [www.sciencedirect.com](http://www.sciencedirect.com)journal homepage: [www.ejconline.com](http://www.ejconline.com)

# Bortezomib-mediated proteasome inhibition as a potential strategy for the treatment of rhabdomyosarcoma

Francesca Bersani<sup>a,b</sup>, Riccardo Taulli<sup>a,b</sup>, Paolo Accornero<sup>c</sup>, Alessandro Morotti<sup>d</sup>,  
Silvia Miretti<sup>c</sup>, Tiziana Crepaldi<sup>a,b</sup>, Carola Ponzetto<sup>a,b,\*</sup>

<sup>a</sup>Center for Experimental Research and Medical Studies (CeRMS), University of Torino, Torino, Italy

<sup>b</sup>Department of Anatomy, Pharmacology and Forensic Medicine, University of Torino, C.so Massimo D'Azeglio 52, 10126 Torino, Italy

<sup>c</sup>Department of Veterinary Morphophysiology, University of Torino, Grugliasco, Italy

<sup>d</sup>Department of Clinical and Biological Sciences, San Luigi Hospital, Orbassano, Italy

## ARTICLE INFO

### Article history:

Received 21 November 2007

Received in revised form

7 February 2008

Accepted 12 February 2008

Available online 14 March 2008

### Keywords:

Rhabdomyosarcoma

Bortezomib

Proteasome

Novel cancer therapies

## ABSTRACT

Rhabdomyosarcoma (RMS) is the most common soft-tissue sarcoma of childhood, divided into two major histological subtypes, embryonal (ERMS) and alveolar (ARMS). To explore the possibility that the proteasome could be a target of therapeutic value in rhabdomyosarcoma, we treated several RMS cell lines with the proteasome inhibitor bortezomib (Velcade or PS-341) at a concentration of 13–26 nM. RMS cells showed high sensitivity to the drug, whereas no toxic effect was observed in primary human myoblasts. In both ERMS and ARMS cells bortezomib promoted apoptosis, activation of caspase 3 and 7 and induced a dose-dependent reduction of anchorage-independent growth. Furthermore, bortezomib induced activation of the stress response, cell cycle arrest and the reduction of NF- $\kappa$ B transcriptional activity. Finally, bortezomib decreased tumour growth and impaired cells viability, proliferation and angiogenesis in a xenograft model of RMS. In conclusion, our data indicate that bortezomib could represent a novel drug against RMS tumours.

© 2008 Elsevier Ltd. All rights reserved.

## 1. Introduction

The proteasome is a large enzyme complex responsible for ubiquitin-mediated protein degradation and maintenance of homeostasis in eukaryotic cells. It is primarily involved in the degradation of misfolded and short-lived regulatory proteins essential for cell cycle progression, apoptosis and signal transduction.<sup>1</sup> Malignant cells, which frequently harbour mutations in cell cycle and apoptotic checkpoints, have an increased dependency on proteasome-mediated degradation of aberrant proteins. Accordingly, tumour cells are much more sensitive to proteasome inhibitors than normal cells.<sup>2</sup> This and the consequent tolerable therapeutic index

make the proteasome a novel and promising target for cancer treatment.<sup>1</sup>

Bortezomib (or Velcade or PS-341), a dipeptidyl boronic acid derivative, is a highly selective and reversible inhibitor of the chymotryptic-like activity of the 26S proteasome subunit. Amongst the proteasome inhibitors, bortezomib is the most specific and the only one with no additional targets reported to date.<sup>3</sup> Bortezomib can promote apoptosis in tumour cells through multiple mechanisms, including stabilisation of pro-apoptotic proteins and cyclin-dependent kinase inhibitors, induction of G<sub>2</sub>/M cell cycle arrest, activation of the stress response and inhibition of the NF- $\kappa$ B signalling pathway.<sup>1</sup> Bortezomib, already approved by the Food and Drug

\* Corresponding author. Address: Department of Anatomy, Pharmacology and Forensic Medicine, University of Torino, C.so Massimo D'Azeglio 52, 10126 Torino, Italy. Tel.: +39 011 6707799; fax: +39 011 6705931.

E-mail address: [carola.ponzetto@unito.it](mailto:carola.ponzetto@unito.it) (C. Ponzetto).

0959-8049/\$ - see front matter © 2008 Elsevier Ltd. All rights reserved.

doi:10.1016/j.ejca.2008.02.022

Administration for the treatment of relapsed and refractory multiple myeloma,<sup>4</sup> is currently undergoing clinical trials for various forms of cancer, including different solid tumours.<sup>5</sup>

Soft tissue sarcomas constitute the sixth most common malignancy in childhood. Among them, rhabdomyosarcoma (RMS) stands out as the first one and as the third most common in the adult.<sup>6</sup> RMS is a heterogeneous tumour, expressing skeletal muscle-specific markers. The two major categories of RMS are of embryonal (ERMS) and alveolar (ARMS) histologies. ARMS is the rarest<sup>7</sup> but the most aggressive type, with a higher trend to metastasize.<sup>8</sup> It predominantly arises in adolescents and young adults, whereas ERMS usually occurs in paediatric patients. Whilst intensive combined treatments have significantly improved the prognosis of patients with local disease, for metastatic RMS the 5-year failure-free survival has remained at around 40%, with a worse outcome for the alveolar subtype.<sup>8</sup> A major limiting factor in RMS treatment is the intrinsic and/or acquired resistance to chemo- and radiation-therapy<sup>9</sup> with frequent recurrence.

It has been shown that the proteasome inhibitor lactacystin has some differentiative activity on an ERMS-derived cell line.<sup>10</sup> A recent phase I study aimed at determining toxicity and pharmacodynamics of bortezomib in paediatric patients with refractory solid tumours included two cases of RMS and highlighted its good tolerability in children.<sup>11</sup> The prerequisite to explore the applicability of this novel agent in paediatric solid tumours therapy is further preclinical investigation of its efficacy in RMS cell lines.

In the present study, we examined the antitumour activity of bortezomib on five RMS cell lines and found it highly efficient in inducing apoptosis, anchorage-independent growth inhibition and growth arrest, whereas it was without effect on primary human myoblasts used as control. We also showed that bortezomib inhibits tumour growth in xenografts of both ERMS and ARMS. Altogether, our findings demonstrate that RMS cells are sensitive to bortezomib both *in vitro* and *in vivo* and suggest a possible use of bortezomib for the treatment of this disease.

## 2. Materials and methods

### 2.1. Reagents

All reagents, unless specified, were from Sigma-Aldrich (St. Louis, MO).

### 2.2. Cell cultures

Human RMS cells of embryonal (RD, their subclone RD18 and CCA) and alveolar (Sj-RH30 and Sj-RH4) histotype, kindly provided by Dr. Pier Luigi Lollini (Department of Experimental Pathology, University of Bologna, Italy) and primary human myoblasts, kindly provided by Dr. Susan Treves (Departments of Anaesthesia and Research, Basel University Hospital, Switzerland) were grown in DMEM (Euroclone, Pero, Italy) supplemented with 10% foetal bovine serum (FBS; Euroclone). Jurkat cells were grown in RPMI (Euroclone) supplemented with 10% FBS. All cells were incubated at 37 °C in a 7% CO<sub>2</sub>-water-saturated atmosphere and media were supplemented with 2 mM L-glutamine, 100 U penicillin and 0.1 mg/ml streptomycin.

### 2.3. Drugs

The proteasome inhibitor bortezomib, a gift of Millennium Pharmaceuticals (Cambridge, MA), was dissolved in DMSO at a stock concentration of 26 µM and stored at –80 °C. Fresh dilutions in medium were made for each experiment. An equal amount of DMSO was used as control in all untreated samples (NT). Tumour necrosis factor-α (TNFα) was purchased from MP Biomedicals (Solon, OH).

### 2.4. Assessment of apoptosis

Apoptosis was measured by flow cytometry after staining with Annexin V or with the mitochondrion-permeable voltage-sensitive dye tetramethylrhodamine methyl ester (TMRM; Molecular Probes, Eugene, OR) for Sj-RH4 cells. Briefly, after exposure to bortezomib, cells ( $1 \times 10^5$ ) were trypsinised, washed in PBS, and incubated for 15 min at 37 °C in HEPES buffer solution [10 mmol/l HEPES (pH 7.4), 140 mmol/l NaCl, 2.5 mmol/l CaCl<sub>2</sub>] with 2.5 µl biotin-conjugated annexin V (BD PharMingen Biosciences, San Diego, CA) or with 200 nM TMRM. Annexin V binding was revealed by additional incubation with 0.5 µl streptavidin-allophycocyanin (APC; BD PharMingen Biosciences). Cells were analysed by FACScan using CellQuest Software (BD PharMingen Biosciences).

### 2.5. Western blot

Cells were washed with ice-cold PBS, lysed and scraped in lysis buffer [20 mmol/l Tris (pH 7.5), 150 mmol/l NaCl, 1 mmol/l EDTA, 1 mmol/l EGTA, 1% Triton X-100, 1 mmol/l β-glycerolphosphate] with Protease Inhibitor Cocktail and 1 mmol/l sodium-orthovanadate. Protein lysates were cleared of cellular debris by centrifugation at 4 °C for 10 min at 12,000 × *g*, quantified using Bio-Rad (Hercules, CA) protein assay, resolved in 10% SDS-PAGE gels, and transferred to Hybond-C Extra nitrocellulose membranes (Amersham Biosciences, Piscataway, NJ). Proteins were visualised with horseradish peroxidase-conjugated secondary antibodies and Super Signal West Pico Chemiluminescent Substrate (Pierce, Rockford, IL).

### 2.6. Antibodies

Anti-cleaved-caspase 3 (Asp<sup>175</sup>), anti-cleaved-caspase 7 (Asp<sup>198</sup>), anti-phospho-JNK, anti-phospho-p38 MAPK and anti-phospho IκBα (Ser<sup>32</sup>) were from Cell Signaling Technology (Danvers, MA); anti-α-tubulin was from Sigma-Aldrich; anti-p21, anti-p65 and anti-CD31 (PECAM-1) were from Santa Cruz Biotechnology (Santa Cruz, CA); anti-Ki67 was from Novocastra (Newcastle, UK). Anti-ubiquitin antibody was kindly provided by Dr. Michele Pagano (Department of Pathology, New York University, USA).

### 2.7. Cell cycle analysis

Cells were cultured for 0, 12, 24 h in the presence of bortezomib (26 nM). After being harvested and washed with PBS,  $5 \times 10^5$  cells were fixed for 1 min in 70% ice-cold ethanol at 4 °C. After washing, cells were treated with RNase (0.25 mg/

ml) and stained with propidium iodide (50 µg/ml). The cell cycle distribution in G<sub>0</sub>/G<sub>1</sub>, S and G<sub>2</sub>/M phase was calculated using the CellQuest program (BD Pharmingen Biosciences).

## 2.8. Luciferase reporter assay

Cells, plated at a density of  $1 \times 10^5$  per well in 24-well plates, were transfected with the NF-κB-luciferase reporter plasmid previously described<sup>12</sup> using Lipofectamine 2000 reagent (Invitrogen, Carlsbad, CA). Twenty-four hours after transfection, cells were exposed to bortezomib (26 nM) for 12 h. Luciferase activity was determined using the Luciferase Assay System (Promega, Madison, WI).

## 2.9. Evaluation of NF-κB activity

The DNA binding activity of NF-κB in RD18 and Jurkat cells was quantified by enzyme-linked immunosorbent assay (ELISA) using the Trans-AM™ NF-κB p65 Transcription Factor Assay Kit (Active Motif North America, Carlsbad, CA) according to the manufacturer's instructions.

## 2.10. Lentiviral vectors transduction

Cells, plated at a density of  $1 \times 10^5$  per well in 35-mm diameter culture dishes, were transduced with the previously described lentiviral vectors containing either a p53-specific shRNA (LV-shp53) or a mutated control shRNA (LV-shC).<sup>13</sup> The medium was changed 12 h after infection.

## 2.11. Anchorage-independent cell growth assay

Cells were suspended in 0.35% type VII low melting agarose in 10% DMEM at  $2 \times 10^4$  per well and plated on a layer of 0.7% agarose in 10% DMEM in 6-well culture plates and cultured at 37 °C with 7% CO<sub>2</sub>. Bortezomib-containing medium was replaced every 3 days. After 2 weeks, colonies >100 µm in diameter were counted.

## 2.12. Xenograft murine model

RD18 and Sj-RH30 cells were trypsinised and resuspended at  $1 \times 10^7$ /ml in sterile PBS. 100 µl were injected s.c. into the flank of female *nu/nu* mice (Charles River, Wilmington, MA). When the tumours became palpable, mice were divided into two groups for each cell line ( $n = 7$  for RD18 and  $n = 4$  for Sj-RH30) receiving bortezomib or saline, respectively. Bortezomib was administered peritumourally at a dosage of 1.25 mg/kg dissolved in 200 µl of saline twice a week, according to Ref. 14. Tumour dimensions were measured with vernier calipers every 3 days and tumour volumes were calculated as the volume of a sphere. All animal procedures were approved by the Ethical Commission of the University of Torino, Italy, and by the Italian Ministry of Health.

## 2.13. Immunohistochemistry and immunofluorescence

Tumour samples were collected at the end of a one-month treatment, fixed and embedded in paraffin. Sections were

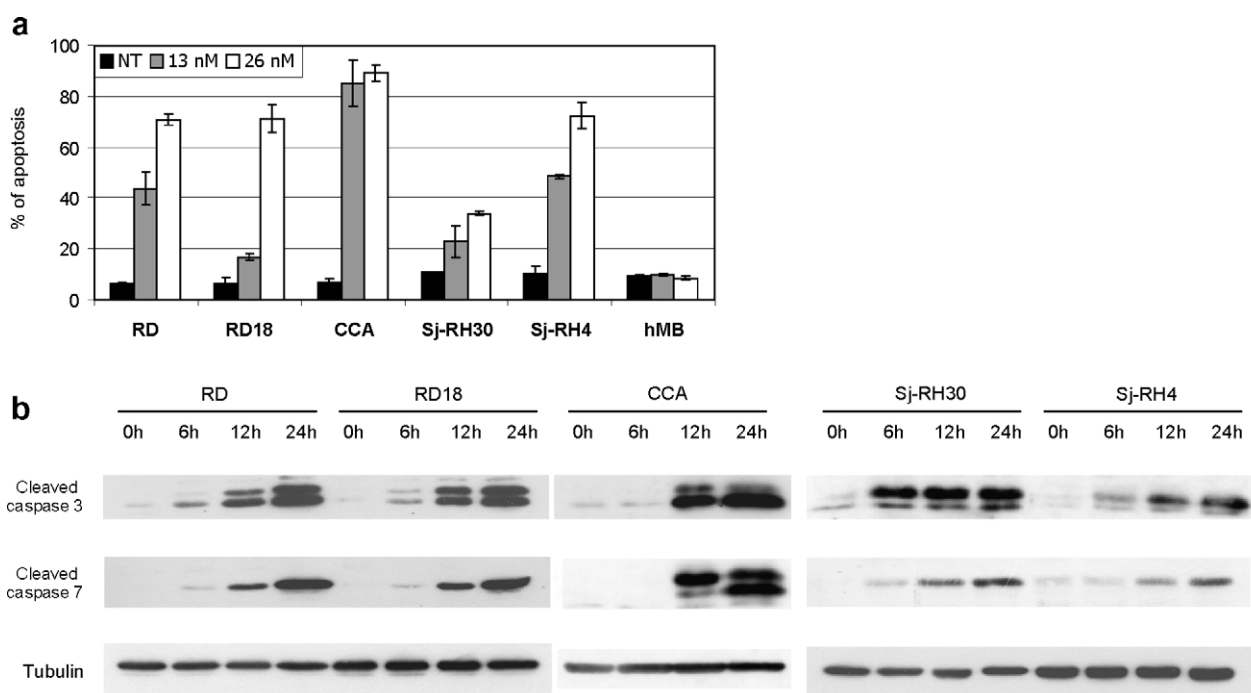


**Fig. 1 – Bortezomib promotes apoptosis and activates the caspases cascade in RMS cell lines.** (a) Cells ( $1 \times 10^5$ /well on 6-well plates) were cultured for 48 h in the absence (NT) or the presence of bortezomib (13–26 nM). Annexin V-APC or TMRM (Sj-RH4) staining and FACS analysis reveal that the drug is active on malignant cells and without effect on human myoblasts (hMB). Mean values ( $\pm$ SD) are from three independent experiments performed in triplicate. (b) Western blot analysis of cleaved-caspase 3, cleaved-caspase 7 and tubulin in lysates (50 µg/lane) of all RMS cell lines treated with bortezomib (26 nM) for the indicated times.

rehydrated and subjected to two antigen retrieval cycles in microwave oven in citrate buffer (pH 6). After blocking for 1 h at room temperature with 0.1% Triton X-100 and 10% normal goat serum in PBS, the sections were incubated with primary antibodies in the same solution at room temperature overnight. Primary antibodies were added at a dilution of 1:300. Sections were further processed with biotinylated secondary antibodies (1:300) and the avidin–biotin–peroxidase complex (ABC, Vector, Burlingame, CA) and finally visualised with 3,3'-diaminobenzidine (Roche, Indianapolis, IN). Immunofluorescence on the collected tumours was performed as described in Ref. 15. Anti-CD31 antibody was diluted 1:200. Cell nuclei were stained using DAPI. The number of CD31 positive blood vessels was counted at high power magnification (40×) on five fields from tumours derived from three treated and three control mice.

### 3. Results

#### 3.1. Bortezomib promotes apoptosis in RMS cells

Three ERMS (RD, RD18 and CCA) and two ARMS (Sj-RH30 and Sj-RH4) cell lines were analysed. Bortezomib caused massive

apoptosis in all RMS lines at low nanomolar concentrations, although the sensitivity to the drug varied (Fig. 1a). Overall, ERMS showed higher susceptibility with respect to ARMS. The Sj-RH30 cell line appeared to be the most resistant, but when the treatment was prolonged to 72 h, apoptosis reached levels comparable to those seen in the other cells (data not shown). Bortezomib was without effect when added at the same concentrations to primary human myoblasts (hMB, Fig. 1a).

To characterise the events associated with the lethal effect of bortezomib, RMS cells exposed to the drug for different times were analysed for caspase activation. Western blot with the appropriate antibodies confirmed early cleavage of caspase 3 and 7, occurring just 6 h after exposure to bortezomib (Fig. 1b), when phenotypic changes were not yet detectable.

#### 3.2. Exposure of RMS cells to bortezomib causes enhanced protein ubiquitination, stress response induction, growth arrest and p21 accumulation

To verify the inhibitory effect of the drug on the proteasome, RMS cells were treated with bortezomib and the lysates were probed with an anti-ubiquitin antibody. Time course analysis

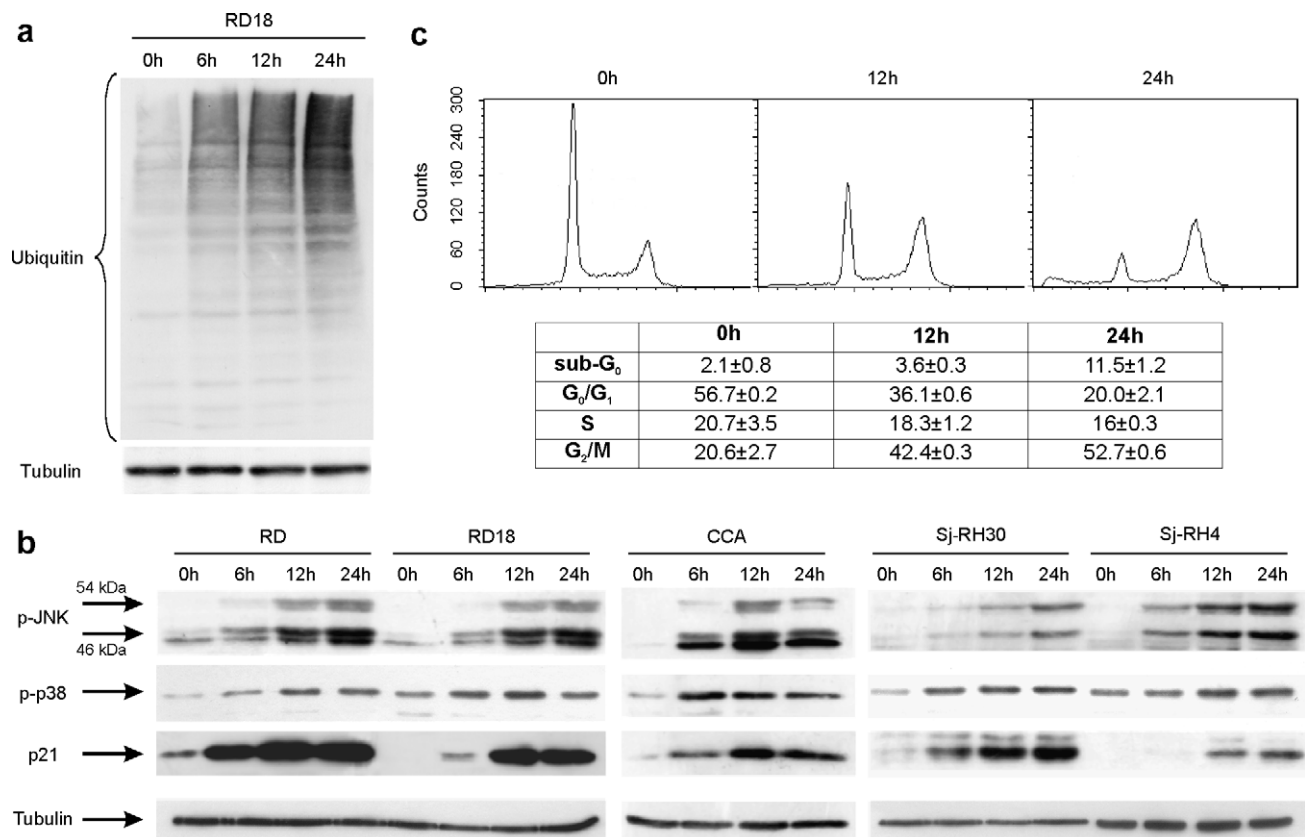


**Fig. 2 – Bortezomib induces polyubiquitinated proteins accumulation, JNK and p38 phosphorylation, increase of p21 levels and G<sub>2</sub>/M cell cycle arrest.** (a) Western blot of ubiquitinated proteins in lysates (50 µg/lane) of RD18 cells treated with 26 nM bortezomib for the indicated times. Tubulin was used as loading control. (b) Western blot of p-JNK, p-p38, p21 and tubulin in lysates of RMS cells exposed to 26 nM bortezomib for the indicated times. Equivalent amounts of lysate (30 µg/lane) were loaded in each lane. (c) Cell cycle distribution of RD18 cells treated with bortezomib (26 nM) was analysed by propidium iodide (PI) staining and FACS analysis after 0, 12 and 24 h of culture. For each sample, the percentage of cells in sub-G<sub>0</sub>, G<sub>0</sub>/G<sub>1</sub>, S and G<sub>2</sub>/M phase is indicated (±SD of three independent experiments).

showed a rapid and progressive accumulation of ubiquitinated proteins (Fig. 2a).

We then investigated the effects of bortezomib on effector proteins potentially involved in the apoptotic response. Proteasome inhibition-induced activation of c-Jun N-terminal kinase (JNK) and p38 MAPK, both playing a central role in the stress-related pathway and in apoptosis induction, was previ-

ously reported.<sup>16</sup> In RMS cells, phosphorylation of JNK and p38 increased in response to bortezomib, especially at 12–24 h of treatment (Fig. 2b).

To verify the effect of the drug on the division of RMS cells, we analysed their cell cycle distribution after bortezomib treatment. At 12–24 h, there was an increase (more than two-fold) of the cells in G<sub>2</sub>/M phase, with a corresponding decrease in the number of cells in G<sub>0</sub>/G<sub>1</sub> (Fig. 2c). Accordingly, the level of p21 was markedly increased. It should be noted that RD, RD18, Sj-RH30 and Sj-RH4 cells, all responsive to bortezomib, carry mutations in p53 which make it non-functional,<sup>17,18</sup> and that CCA cells do not show any increase in p53 level after bortezomib treatment (data not shown). Thus, bortezomib-induced cell cycle arrest is p53 independent.

### 3.3. Bortezomib inhibits NF- $\kappa$ B in RMS cells thereby contributing to apoptosis

NF- $\kappa$ B is a transcription factor which regulates a wide range of biological processes (including cell growth and protection from apoptosis) and is frequently hyper-activated in tumours.<sup>19</sup> One of the major effects of proteasome inhibition is the reduction of NF- $\kappa$ B activity due to the accumulation of phospho-I $\kappa$ B $\alpha$  which retains NF- $\kappa$ B in the cytosol.<sup>19</sup> Bortezomib treatment indeed increased phospho-I $\kappa$ B $\alpha$  in RMS cells (Fig. 3a). Consistent with this, in RD18 cells, bortezomib caused nearly 50% inhibition of both the basal NF- $\kappa$ B DNA binding and transcriptional activity (Fig. 3b–c).

To verify whether the induction of apoptosis observed in RMS cells upon bortezomib treatment was linked to NF- $\kappa$ B inhibition, we used RNA interference to downregulate the p65 subunit of NF- $\kappa$ B.<sup>13</sup> RD18 cells were transduced with a lentiviral vector containing either a shRNA against p65

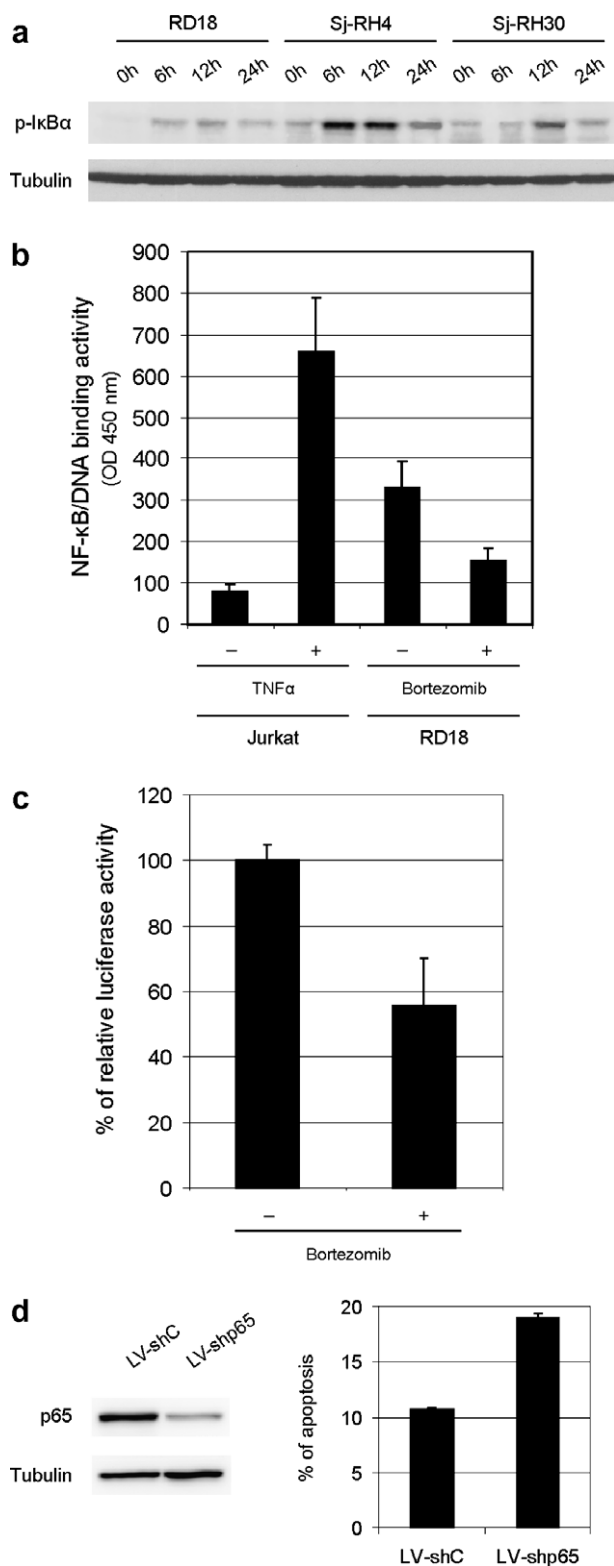


**Fig. 3 – Bortezomib induces the accumulation of p-I $\kappa$ B $\alpha$  and the reduction of NF- $\kappa$ B transcriptional activity and NF- $\kappa$ B contributes to the induction of apoptosis.** (a) Western blot of p-I $\kappa$ B $\alpha$  and tubulin in extracts of RMS cells exposed to 26 nM bortezomib for the indicated times. 50  $\mu$ g of lysate were loaded in each lane. (b) To determine NF- $\kappa$ B/DNA binding activity, extracts (20  $\mu$ g) from RD18 and Jurkat cells (used as negative and positive control) were analysed using an ELISA kit. RD18 cells were treated for 12 h with 26 nM bortezomib; Jurkat cells were stimulated for 15 min with 100 ng/ml TNF $\alpha$ . Bars indicate SD of three independent experiments. (c) RD18 cells were transfected with an NF- $\kappa$ B-luciferase reporter construct and, after 24 h, either treated with 26 nM bortezomib or left untreated (NT). Luciferase activity was assayed 12 h later. Results are expressed as relative percentage of untreated cells, set at 100%. Mean values ( $\pm$ SD) are from three independent experiments performed in duplicate. (d) Left: RD18 cells transduced with the LV-shp65 or the mutated control LVshC were immunoblotted with antibodies anti-p65 and tubulin as a loading control. Right: cells were harvested 72 h post-infection, stained with Annexin V-APC and apoptosis was measured by FACS analysis. Mean values ( $\pm$ SD) are from three independent experiments.



(LV-shp65) or a control shRNA (LV-shC) and 72 h later p65 levels were strongly downregulated in the cells infected with LV-shp65 (Fig. 3d, left panel). Annexin V staining of the p65-depleted cells followed by FACS analysis revealed an increase in the percentage of apoptotic cells compared to those transfected with the control vector (Fig. 3d, right panel). Thus, NF- $\kappa$ B inhibition is likely to contribute to bortezomib-mediated apoptosis in RMS cells.

### 3.4. Bortezomib inhibits anchorage-independent growth of RMS cells

We next examined if bortezomib-mediated proteasome inhibition could affect anchorage-independent growth of RMS cells. Growth in soft agar was significantly inhibited in a dose-dependent manner by bortezomib (Fig. 4a and b). A dosage of 11.5 nM was sufficient to cause a ~50% reduction in the number of colonies in all cell lines. It should be noted that this concentration of the drug induced only ~25% apoptosis in the same cells growing on plastic (data not shown). Thus, even in the more resistant ARMS cells, bortezomib interfered with the transformed phenotype without requiring concentrations necessary to induce cell death.

### 3.5. Bortezomib inhibits tumour growth by impairing cells viability, proliferation and angiogenesis in a xenograft model of RMS

To determine whether bortezomib treatment could have an effect on tumour growth *in vivo*, we generated xenograft models of RMS by injecting either RD18 (ERMS) or Sj-RH30 (ARMS) cells *s.c.* into nude mice. As tumours became palpable (indi-

cated as day 0), two groups of mice were treated with bortezomib at 1.25 mg/kg twice a week<sup>14</sup> for one month, whilst control mice received vehicle alone. In both cases (ERMS and ARMS) the treatment resulted in an evident reduction of tumour growth, without any obvious side-effect, except for a minimal weight loss (Fig. 5a and data not shown).

To investigate the consequences of bortezomib treatment at the cellular level, tumour sections were stained with an anti-cleaved-caspase 3 antibody. The number of positive cells was much higher in the tumours of the treated mice than in the controls (Fig. 5b, upper panels). Higher apoptosis was concomitant with lower proliferation, as shown by a striking reduction of Ki-67-positive cells in the treated tumours (Fig. 5b, lower panels). To verify whether an impairment in angiogenesis also contributed to the slower growth rate of the tumours, the sections were stained with the endothelial marker CD31 and the number of blood vessels was counted. This quantitative analysis showed a significant decrease in vessels density in the tumours of the mice treated with bortezomib as compared to controls (Fig. 5c).

Altogether these data suggest that apoptosis, decreased proliferation and reduced angiogenesis may represent possible mechanisms to explain the antitumourigenic action of bortezomib in RMS.

## 4. Discussion

Embryonal and alveolar rhabdomyosarcomas represent a therapeutic challenge because of their prevalence in children and frequent resistance to conventional chemotherapy. It is known that the etiology of the two types of RMS is different. In fact, whilst ARMS is caused by the PAX3/PAX7-FHFR

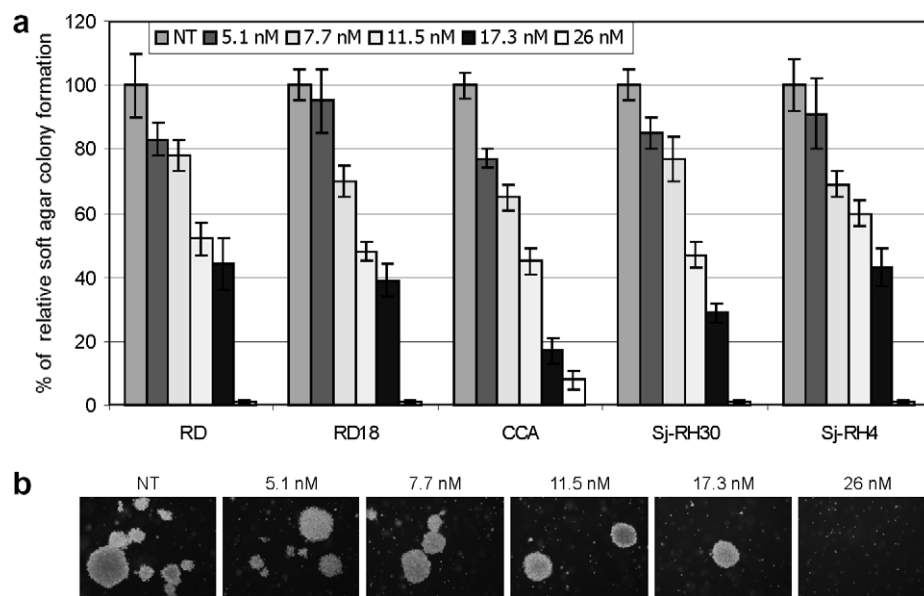


**Fig. 4 – Bortezomib inhibits anchorage-independent growth of embryonal and alveolar RMS cell lines. (a)** Soft agar growth was evaluated by resuspending RMS cells ( $2 \times 10^4$ /well in 6-well plates) in 0.35% agar. RMS cells were cultured in two layers of soft agar with the indicated concentrations of bortezomib, and colonies were counted 2 weeks later. Medium with fresh drug was replaced every 3 days. The number of colonies obtained from untreated cells (NT) was set at 100%. Mean values ( $\pm$ SD) are from three independent experiments performed in triplicate. **(b)** Pictures are representative results of the colony formation assay for Sj-RH30 cells.

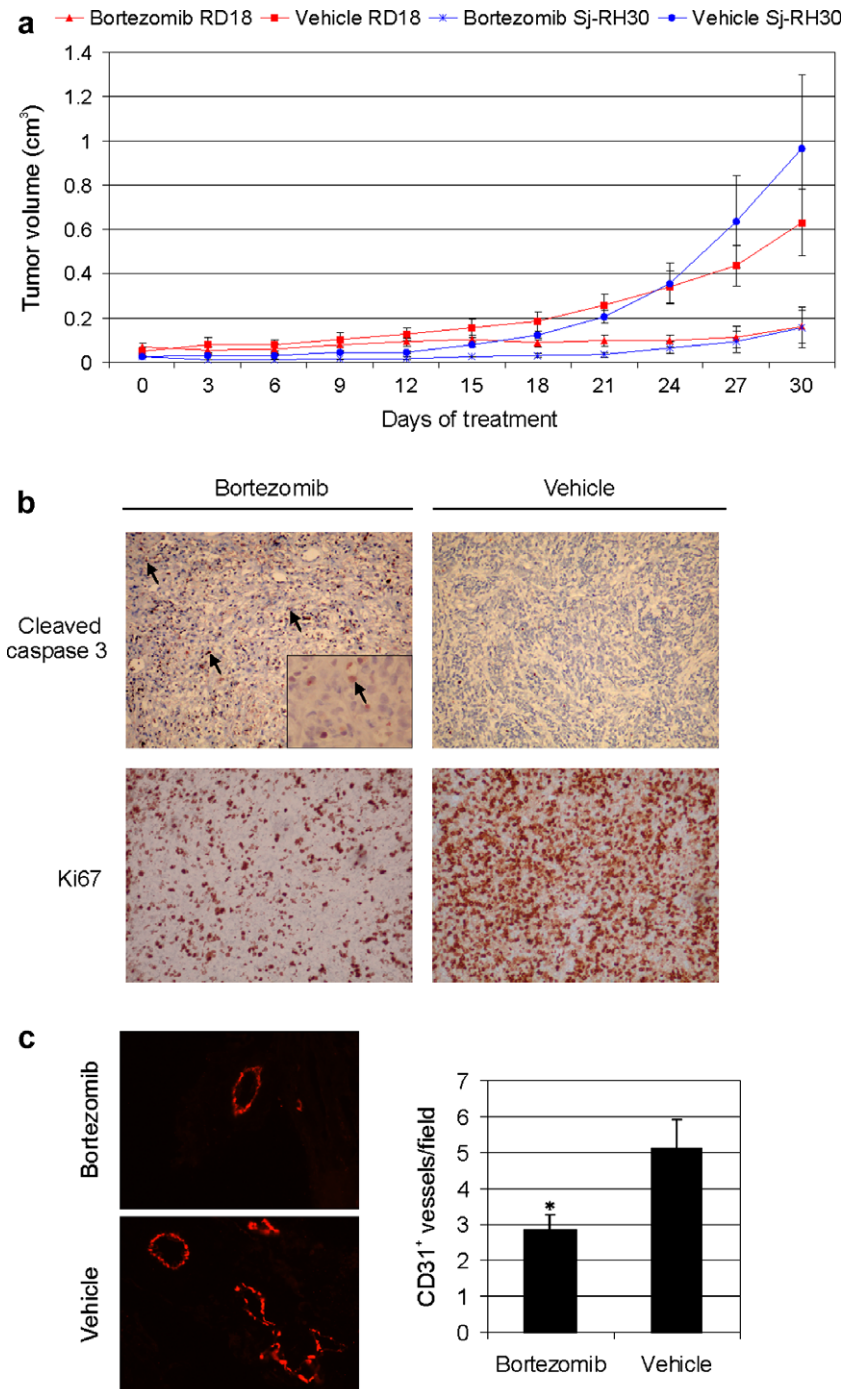


**Fig. 5 – Bortezomib inhibits the growth of tumours derived from xenografts of RD18 (ERMS) and Sj-RH30 (ARMS) cells in nude mice. (a)** Tumour growth was evaluated by injecting animals s.c. with  $1 \times 10^6$  RD18 or Sj-RH30 cells. When tumours were palpable, half of the mice were treated twice a week with 1.25 mg/kg bortezomib for one month, whilst the other half received saline alone (Vehicle). Tumour growth was measured every three days. Bars indicate SD. **(b)** Upper panels: representative anti cleaved-caspase 3 immunohistochemistry on the RD18 xenografts. Arrows show positive cells. Lower panels: Ki67 staining on the same RD18 xenografts. **(c)** Left: immunofluorescence with anti-CD31 antibody in sections of tumours derived from RD18 xenografts. High power fields are shown. Right: quantification of microvessels stained with CD31-specific antibody. The density is expressed as counts from 5 fields per tumour from three tumours for each group. Bars indicate SD. \* $P < 0.03$  versus control.

translocation, no specific genetic abnormality has been yet identified in ERMS.<sup>6</sup> Furthermore, expression profiling has confirmed that the transcriptional signatures of the two

tumours differ widely.<sup>20</sup> Considering that the trend to metastasize is typical of the alveolar subtype, the search for novel treatments could be aimed at subtype-specific targets.

However, it seemed to us that in the absence of molecularly-targeted compounds, bortezomib, the only proteasome inhibitor so far approved by the FDA as an anti-cancer drug, could be worth of consideration as a possible therapeutic tool. A recent phase II study has shown that bortezomib has a very limited efficacy as a single agent on adults with recurrent or metastatic sarcomas,<sup>21</sup> but others suggest that it could be of value in combination treatments.<sup>5,14</sup> Interestingly, a phase I study indicates that bortezomib is particularly well tolerated by children.<sup>11</sup>

To explore the therapeutic potential of bortezomib in RMS, we investigated its effects in both ERMS and ARMS cell lines. We found that all RMS cell lines, regardless of the histological subtype, were highly sensitive to bortezomib and that nanomolar concentrations of the drug were sufficient to induce cell death. Bortezomib stimulated high levels of apoptosis with concomitant cleavage of caspases in all RMS cell lines tested, although ERMS displayed higher sensitivity than ARMS cells. Moreover, this effect appeared to be specific for transformed cells because no toxicity was observed in primary human myoblasts exposed to the drug. These results suggest that bortezomib treatment of RMS patients should not cause side-effects on healthy muscle tissue.

As expected,<sup>22,23</sup> bortezomib stimulated phosphorylation of JNK and increased phosphorylation of p38 in RMS cells. However, the specific inhibition of either one or both kinases was not sufficient to prevent apoptosis (data not shown), suggesting that the induction of the stress response is just one of the multiple cytotoxic effects that bortezomib elicits in RMS cells.

Consistent with reports on its effects on other cell types,<sup>4,23,24</sup> bortezomib induced cell cycle arrest in RMS cells. Considering that four out of the five cell lines analysed were p53 mutated<sup>17,18</sup> and that in only one with a potentially wild type p53 its level was unchanged, this block must occur in a p53-independent way. On the other hand, we found that bortezomib induced up-regulation of p21 and downregulation of cdc25c (not shown), which could themselves play a major role in mediating G<sub>2</sub>/M cell cycle arrest.<sup>25</sup>

One of the pathways best known for being affected by proteasome inhibitors is the nuclear translocation and transcriptional activation of NF- $\kappa$ B.<sup>4,23,26</sup> Our results show that in RMS cells bortezomib treatment did induce an accumulation of phosphorylated-I $\kappa$ B $\alpha$  resulting in the reduction of the NF- $\kappa$ B/DNA-binding and transcriptional activity. Accordingly, knockdown of the p65 subunit of NF- $\kappa$ B by RNA interference resulted in apoptosis induction, thus suggesting that inhibition of NF- $\kappa$ B contributes to the proapoptotic activity of bortezomib in RMS cells.

When bortezomib was tested on RMS cells growing in soft agar, anchorage independence was lost at low nanomolar concentrations which were non-toxic to the cells, indicating that the drug interferes directly with the transformed phenotype. The efficacy of bortezomib was also confirmed *in vivo*, in nude mice bearing RMS xenografts, where treatment with the drug caused significant inhibition of tumour growth. Importantly, the treated tumours were less vascularised than those of the controls.

Our results may be of clinical interest for two reasons. First, they show that bortezomib causes significant RMS cells

apoptosis in a p53 independent way. Given that the p53 tumour suppressor is frequently mutated in children with RMS,<sup>17,27</sup> our results indicate that the absence of a functionally active p53 protein would not compromise a bortezomib-based therapy. Second, consistent with the analogous data obtained on other tumour types,<sup>14,28,29</sup> the reduction of tumour microvasculature observed in our model might contribute to the induction of apoptosis even in tumours that are refractory to the direct cytotoxic effects of the drug. Altogether our results should encourage further clinical studies of bortezomib in RMS, especially in the absence of approved molecularly targeted compounds active on the more aggressive forms of this childhood malignancy.

## Conflict of interest statement

None declared.

## Acknowledgements

We thank Millennium Pharmaceuticals for supplying bortezomib, Dr. Roberto Chiarle for his precious help with the immunohistochemistry and Dr. Roberto Piva and Dr. Giorgio Inghirami for useful advice. We are grateful to Dr. Pier Luigi Lollini for the rhabdomyosarcoma cell lines, to Dr. Susan Treves for the primary human myoblasts and to Dr. Michele Pagano for the anti-ubiquitin antibody. This work was supported by funding under the Italian Association for Cancer Research (CP), the Oncology Project Compagnia di San Paolo/FIRMS (CeRMS), Regione Piemonte-Ricerca Sanitaria Finalizzata and the Sixth Research Framework Programme of the European Union, Project RIGHT (LSHB-CT-2004-005276).

## REFERENCES

- Adams J. The proteasome: a suitable antineoplastic target. *Nat Rev Cancer* 2004;**4**:349–60.
- Almond JB, Cohen GM. The proteasome: a novel target for cancer chemotherapy. *Leukemia* 2002;**16**:433–43.
- Crawford LJ, Walker B, Ovaa H, et al. Comparative selectivity and specificity of the proteasome inhibitors BzLLCCHO, PS-341, and MG-132. *Cancer Res* 2006;**66**:6379–86.
- Hideshima T, Richardson P, Chauhan D, et al. The proteasome inhibitor PS-341 inhibits growth, induces apoptosis, and overcomes drug resistance in human multiple myeloma cells. *Cancer Res* 2002;**61**:3071–6.
- Milano A, Iaffaioli RV, Caponigro F. The proteasome: a worthwhile target for the treatment of solid tumors? *Eur J Cancer* 2007;**43**:1125–33.
- Merlino G, Helman LJ. Rhabdomyosarcoma – working out the pathways. *Oncogene* 1999;**18**:5340–8.
- Slater O, Shipley J. Clinical relevance of molecular genetics to paediatric sarcomas. *J Clin Pathol* 2007;**60**:1187–94.
- Wachtel M, Runge T, Leuschner I, et al. Subtype and prognostic classification of rhabdomyosarcoma by immunohistochemistry. *J Clin Oncol* 2006;**24**:816–22.
- Kuttesch Jr JF. Multidrug resistance in pediatric oncology. *Invest New Drugs* 1996;**14**:55–67.
- Mugita N, Honda Y, Nakamura H, et al. The involvement of proteasome in myogenic differentiation of murine myocytes



- and human rhabdomyosarcoma cells. *Int J Mol Med* 1999;3:127–37.
11. Blaney SM, Bernstein M, Neville K, et al. Phase I study of the proteasome inhibitor bortezomib in pediatric patients with refractory solid tumors: a Children's Oncology Group study (ADVL0015). *J Clin Oncol* 2004;22:4804–9.
  12. Muller M, Morotti A, Ponzetto C. Activation of NF-kappaB is essential for hepatocyte growth factor-mediated proliferation and tubulogenesis. *Mol Cell Biol* 2002;22:1060–72.
  13. Piva R, Gianferretti P, Ciucci A, Taulli R, Belardo G, Santoro MG. 15-Deoxy-delta 12,14-prostaglandin J2 induces apoptosis in human malignant B cells: an effect associated with inhibition of NF-kappa B activity and down-regulation of antiapoptotic proteins. *Blood* 2005;105:1750–8.
  14. Amiri KI, Horton LW, LaFleur BJ, Sosman JA, Richmond A. Augmenting chemosensitivity of malignant melanoma tumors via proteasome inhibition: implication for bortezomib (VELCADE, PS-341) as a therapeutic agent for malignant melanoma. *Cancer Res* 2004;64:4912–8.
  15. De Palma M, Venneri MA, Roca C, Naldini L. Targeting exogenous genes to tumor angiogenesis by transplantation of genetically modified hematopoietic stem cells. *Nat Med* 2003;9:789–95.
  16. Meriin AB, Gabai VL, Yaglom J, Shifrin VI, Sherman MY. Proteasome inhibitors activate stress kinases and induce Hsp72. Diverse effects on apoptosis. *J Biol Chem* 1998;273:6373–9.
  17. Ganjavi H, Gee M, Narendran A, Freedman MH, Malkin D. Adenovirus-mediated p53 gene therapy in pediatric soft-tissue sarcoma cell lines: sensitization to cisplatin and doxorubicin. *Cancer Gene Ther* 2005;12:397–406.
  18. Petitjean A, Mathe E, Kato S, et al. Impact of mutant p53 functional properties on TP53 mutation patterns and tumor phenotype: lessons from recent developments in the IARC TP53 database. *Hum Mutat* 2007;28:622–9.
  19. Karin M, Cao Y, Greten FR, Li ZW. NF-kappaB in cancer: from innocent bystander to major culprit. *Nat Rev Cancer* 2002;2:301–10.
  20. Wachtel M, Dettling M, Koscielniak E, et al. Gene expression signatures identify rhabdomyosarcoma subtypes and detect a novel t(2;2)(q35;p23) translocation fusing PAX3 to NCOA1. *Cancer Res* 2004;64:5539–45.
  21. Maki RG, Kraft AS, Scheu K, et al. A multicenter Phase II study of bortezomib in recurrent or metastatic sarcomas. *Cancer* 2005;103:1431–8.
  22. Hideshima T, Mitsiades C, Akiyama M, et al. Molecular mechanisms mediating antimyeloma activity of proteasome inhibitor PS-341. *Blood* 2003;101:1530–4.
  23. Yin D, Zhou H, Kumagai T, et al. Proteasome inhibitor PS-341 causes cell growth arrest and apoptosis in human glioblastoma multiforme (GBM). *Oncogene* 2005;24:344–54.
  24. Ling YH, Liebes L, Jiang JD, et al. Mechanisms of proteasome inhibitor PS-341-induced G(2)-M-phase arrest and apoptosis in human non-small cell lung cancer cell lines. *Clin Cancer Res* 2003;9:1145–54.
  25. Hideshima T, Chauhan D, Ishitsuka K, et al. Molecular characterization of PS-341 (bortezomib) resistance: implications for overcoming resistance using lysophosphatidic acid acyltransferase (LPAAT)-beta inhibitors. *Oncogene* 2005;24:3121–9.
  26. Sors A, Jean-Louis F, Pellet C, et al. Down-regulating constitutive activation of the NF-kappaB canonical pathway overcomes the resistance of cutaneous T-cell lymphoma to apoptosis. *Blood* 2006;107:2354–63.
  27. Diller L, Sexsmith E, Gottlieb A, Li FP, Malkin D. Germline p53 mutations are frequently detected in young children with rhabdomyosarcoma. *J Clin Invest* 1995;95:1606–11.
  28. Nawrocki ST, Bruns CJ, Harbison MT, et al. Effects of the proteasome inhibitor PS-341 on apoptosis and angiogenesis in orthotopic human pancreatic tumor xenografts. *Mol Cancer Ther* 2002;1:1243–53.
  29. Williams S, Pettaway C, Song R, Papandreou C, Logothetis DJ, McConkey DJ. Differential effects of the proteasome inhibitor bortezomib on apoptosis and angiogenesis in human prostate tumor xenografts. *Mol Cancer Ther* 2003;2:835–43.